

Discovery and Optimization of p38 Inhibitors via Computer-Assisted Drug Design

Daniel R. Goldberg,^{*,†} Ming-Hong Hao,^{*,†} Kevin C. Qian,[†] Alan D. Swinamer,[†] Donghong A. Gao,[†] Zhaoming Xiong,[†] Chris Sarko,[†] Angela Berry,[†] John Lord,[†] Ronald L. Magolda,^{†,‡} Tazmeen Fadra,[†] Rachel R. Kroe,[§] Alison Kukulka,[†] Jeffrey B. Madwed,^{||} Leslie Martin,[†] Christopher Pargellis,[⊥] Donna Skow,[†] Jinhua J. Song,[#] Zhulin Tan,[#] Carol A. Torcellini,[○] Clare S. Zimmitti,^{||} Nathan K. Yee,[#] and Neil Moss[†]

Departments of Medicinal Chemistry, Immunology and Inflammation, Biological and Biomolecular Sciences, Cardiovascular, Drug Discovery Support, and Chemical Development, Boehringer Ingelheim Pharmaceuticals, Inc., Research and Development Center, 900 Ridgebury Road, Ridgefield, Connecticut 06877

Received April 6, 2007

Integration of computational methods, X-ray crystallography, and structure–activity relationships will be disclosed, which lead to a new class of p38 inhibitors that bind to p38 MAP kinase in a Phe out conformation.

Introduction

Mitogen-activated protein kinases (MAPKs) are important components of signal transduction pathways that mediate cell proliferation, differentiation, and death.¹ p38 is a critical member of this family and is important in enabling the production of pro-inflammatory cytokines such as TNF α and IL-1 β , both of which are implicated in chronic inflammatory diseases.² Injectable biologic therapies that bind and inactivate TNF α are effective treatments for rheumatoid arthritis and psoriasis.³ In animal models of arthritis, treatment with p38 inhibitors leads to a reduction in pro-inflammatory cytokine levels and a significant improvement in the severity of inflammation.⁴ Consequently, inhibition of p38 with a small molecule could provide an effective oral therapy for the chronic treatment of these autoimmune diseases.⁵

A number of companies have advanced small molecule p38 inhibitors into the clinic, including ourselves with BIRB 796, **1**.⁶ As part of our efforts to advance the therapeutic potential of p38 inhibition and position ourselves with backup compounds to **1**, we have been seeking alternative classes of inhibitors structurally distinct to **1**. One of the approaches we undertook to accomplish this was to design a new class of p38 inhibitors by capitalizing on the structural perspective we had gained from the X-ray cocrystal structure of **1** bound to p38 and the distinct binding mode revealed by this structure (Figure 1). The binding mode for **1** involves interactions beyond those typically found with many ATP site kinase inhibitors.^{7,8} In addition to the interactions within the adenine binding site and the adjacent kinase specificity pocket, **1** also takes advantage of binding sites made available by the movement of a phenylalanine residue (Phe169) found in the conserved DFG segment of the kinase activation loop. The increased opportunity offered by multiple binding sites for achieving potency encouraged us to focus our design efforts on this Phe out binding mode. Furthermore, the clinical and subsequent commercial success of Imatinib (Gle-

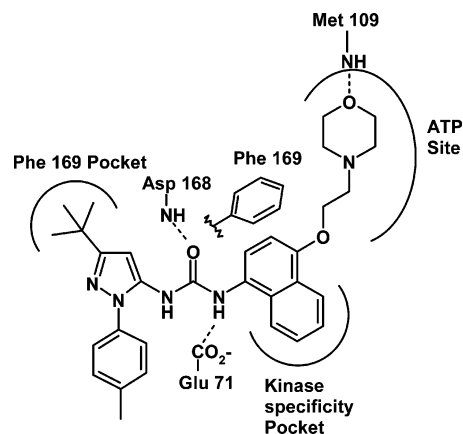


Figure 1. Interactions of **1** in p38.

evac), an Abl kinase inhibitor that also binds in a Phe out binding mode,⁹ helped to reinforce our commitment to the design of new p38 inhibitors that bind in the Phe out binding mode.

Design Process

In considering how best to translate our previously obtained structural information into the design of a new Phe out p38 inhibitor, we felt that computer assisted methods would facilitate the generation of new ideas of how to fill and link between the available binding sites. However, it was not immediately obvious how to design a new group that would ensure binding to p38 in a Phe out manner. We therefore started with a functionality that was already precedented to bind to the region of p38 made available upon the movement of Phe169. For **1**, this functionality includes most notably the *tert*-butyl pyrazole, with the *tert*-butyl group situated tightly in the Phe pocket (the area previously occupied by Phe169 in the Phe in conformation). In addition to this hydrophobic interaction, we felt that two hydrogen bonding interactions were also critical for a Phe out binder, the urea carbonyl with the backbone N–H of Asp168 plus the urea N–H with the carboxyl of Glu71. Previous SAR had demonstrated the essentiality of the urea carbonyl and N–Hs for inhibitor potency in naphthyl urea-based p38 compounds.¹⁰ Furthermore, the observation that other published Phe out inhibitors^{9,11} all contained a related H-bond donor/acceptor arrangement reinforced our belief in the necessity of this type of functionality.

We knew that Phe out fragments structurally distinct from the *tert*-butyl pyrazole functionality in **1** were possible because our own SAR investigations with p38 and that of Bayer with

* To whom correspondence should be addressed. For Daniel R. Goldberg: phone, (203) 778-7828; fax, (203) 791-6072; e-mail, dgoldber@rdg.boehringer-ingelheim.com. For Ming-Hong Hao: phone, (203) 791-6033; fax, (203) 791-6072; e-mail, mhao@rdg.boehringer-ingelheim.com.

[†] Department of Medicinal Chemistry.

[‡] Current Address: Wyeth Research, 865 Ridge Road, Room 1007, Monmouth Junction, NJ 08852.

[§] Department of Biological and Biomolecular Sciences.

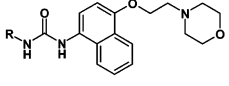
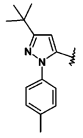
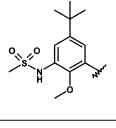
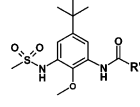
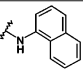
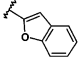
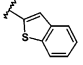
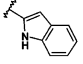
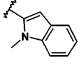
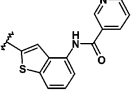
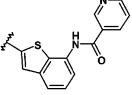
^{||} Department of Cardiovascular Research.

[⊥] Department of Immunology and Inflammation.

[#] Department of Chemical Development.

[○] Department of Drug Discovery Support.

Table 1. Initially Designed Inhibitors

			
Compound	R	T _m (°C) ^{16,a}	Inhibition of TNF α from human whole blood (HuWB) (IC ₅₀ , nM) ^c
Apo p38		47.5	
1		63.0	780
2		60.0	1,065
			
Compound	R'	T _m (°C) ^{16,a}	Inhibition of TNF α from HuWB (IC ₅₀ , nM) ^b
3		56.3	>10,000
4		48.8	>10,000
5		51.4	>10,000
6		49.4 ^b	>10,000
7		51.8	>10,000
8		48.5	>10,000
9		59.5	1,100

^a Values are the mean of \geq two experiments, standard deviation 0.1–0.5 °C unless otherwise noted. ^b Value $n = 1$. ^c Values are the geometric means from 8 to 12 donor experiments, standard deviation typically \pm 50% of reported value.

Sorafenib (Raf inhibitor) revealed that a phenyl template was also a viable option. Table 1 shows one of the more potent phenyl-based alternatives we had found for p38. The *tert*-butyl phenyl sulfonamide derivative **2** (SAR details for this moiety to be published elsewhere) proved essentially equipotent to **1**.¹² As the *tert*-butyl phenyl sulfonamide functionality was structurally distinct from the *tert*-butyl pyrazole functionality in **1**, we chose this group together with the adjacent N–H and carbonyl

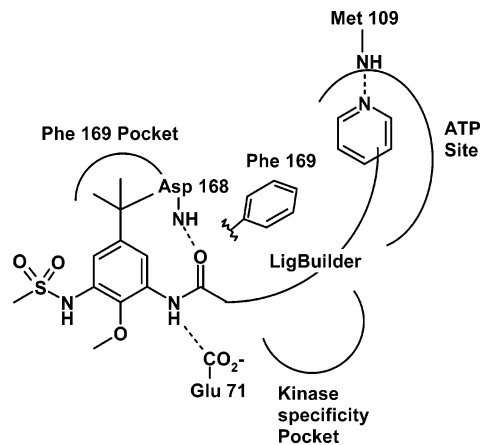


Figure 2. LigBuilder design process.

as a key starting point for applying computer-assisted design to fill the kinase specificity pocket and ATP site in a novel way.

Most potent kinase inhibitors partake in a H-bond with the kinase amino acid that forms an interaction with the N-7 of the adenine ring of ATP;¹³ in the case of p38, this residue is Met109. Given the typical essentiality of this interaction for potent kinase inhibition, we decided to increase our chances of success in applying computer-assisted design by positioning a small fragment to interact with Met109. A common motif in kinase inhibitors associated with this interaction is a pyridine. Thus, we positioned a pyridine group into the ATP site in a typically observed binding orientation. We used the computer program LigBuilder to act as an initial idea generator, utilizing the linking algorithm¹⁴ to generate structures that would link the pyridine to the phenylsulfonamide Phe out fragment with the expectation that the program would use fragments that also take advantage of the kinase specificity pocket (Figure 2).

LigBuilder adds and links fragments from a library of small chemical moieties to generate new structures and then ranks these new structures based on their binding score.¹⁴ LigBuilder generated over 800 different structures bridging the two fragments. However, none of the generated structures were considered ideal, having a high degree of conformational flexibility and not being readily amendable to rapid chemical synthesis. Nonetheless, a common fragment, a 5,6-fused heterocyclic ring, turned up in a significant number of the computationally derived molecules. This observation generated the idea of attaching this fragment directly to the amide of the phenyl sulfonamide group. Computationally, this amide-linked 5,6-fused heterocyclic ring reasonably occupied the kinase specificity pocket. Subsequent modeling identified that a two-atom linker could connect the 5,6-fused heterocyclic ring to the pyridine fragment in the adenine binding site. Based on synthetic flexibility, compound rigidity, and optimal positioning of the pyridine ring to interact with Met109, we chose a carboxamide as a link between the pyridine and the 5,6-fused heterocyclic ring (Figure 3a). Thus, compound **8** became the initial key target to test our design.

Chemistry

Compounds **3–7** were synthesized from commercially available acid or acid chlorides through standard coupling reactions with *tert*-butyl phenyl sulfonamide **25**. To prepare elaborated compounds with the appropriately substituted 4-amino group, the 4-nitrobenzothiophene-2-carboxylic acid **26** was prepared as described in the literature.¹⁵ Coupling of **26** with amine **25** produced amide **27**. Hydrogenation over 10% Pd/C gave **28**, which was then coupled with nicotinic acid to provide **8** (Scheme 1).

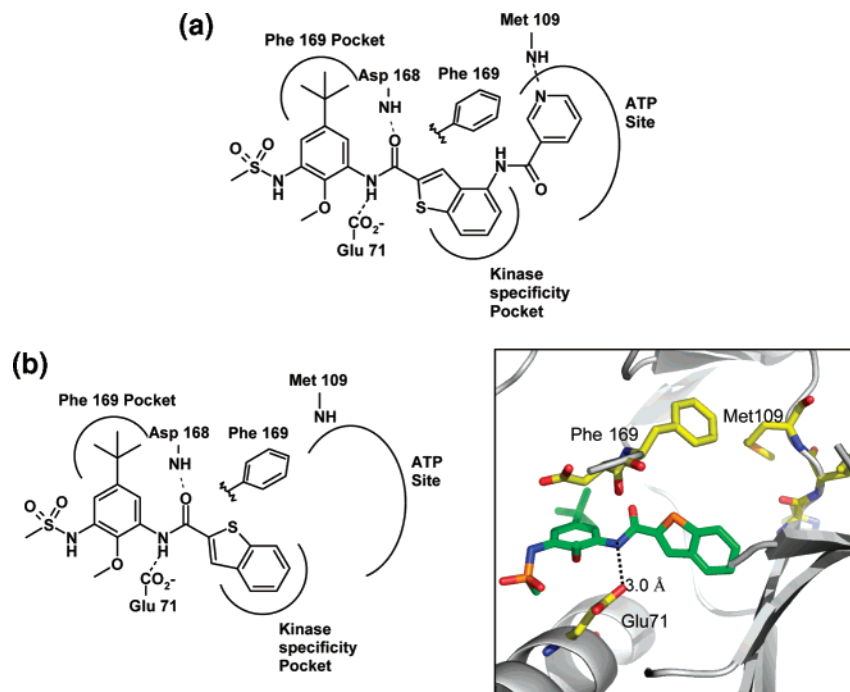
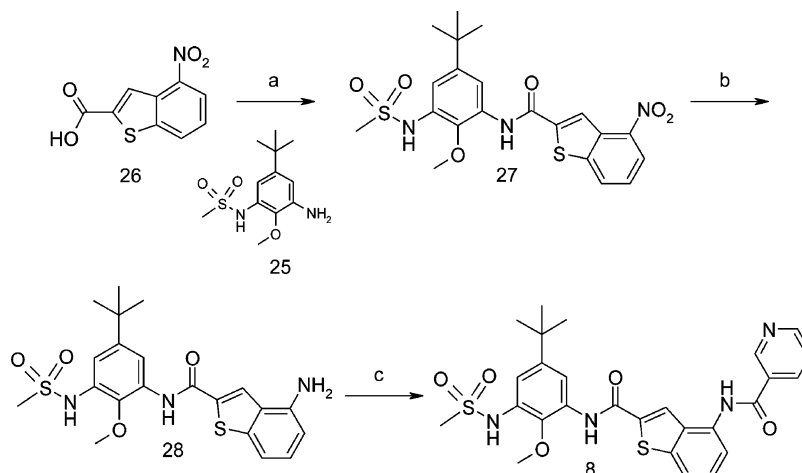


Figure 3. (a) Designed inhibitor **8**. (b) Bound inhibitor and X-ray structure of **5**.

Scheme 1^a



^a Reagents and conditions: (a) TBTU, DIPEA, DMF; (b) H₂, 10% Pd/C, EtOAc; (c) EDC, HOBT, nicotinic acid, DMF.

Compound **9** was prepared from 2-chloro-3-nitrobenzaldehyde **29** (Scheme 2). Addition of the anion of methyl thioglycolate to **29** afforded benzothiophene **30**. Nitro reduction over 10% Pd/C provided **31**. Amide formation with either nicotinic acid or 6-chloronicotinic acid afforded **32** and **33**, respectively, after acid hydrolysis. The amide coupling of carboxylic acids **32** or **33** with aniline **25** gave **9** and **38a**. The *N*-methyl indole core was prepared by methylation of **34** with methyl iodide. Saponification followed by coupling with **25** provided **36**. Subsequent hydrogenation of the nitro group over 10% Pd/C provided **37**, which was coupled with nicotinic acid to provide **10**. Amide formation of **37** with 6-chloronicotinic acid produced **38b**. Nucleophilic substitution of chlorides **38a** or **38b** with both primary and secondary amines provided the compounds listed in Table 2.

Results and Discussion

Before we embarked on the synthesis of designed inhibitor **8**, we prepared truncated analogues containing only the 5,6-heterocycle attached to the phenyl sulfonamide Phe out fragment

to determine if this new way of occupying and linking to the kinase specificity pocket would provide useful binding affinity (Table 1). Somewhat disappointingly, the heterocyclic derivatives **4–7** proved to be over 2 orders of magnitude less potent than the corresponding naphthyl urea **3** based on data from our thermal denaturation assay (Table 1).¹⁶ We nevertheless sought some validation of our original design through preparing the complete compound **8**. Surprisingly, **8** proved to be even less potent ($T_m^a = 48.5$ °C) than the truncated analogue **5** ($T_m = 51.4$ °C). Puzzled by the apparent complete failure of our initial design, we eventually recognized an important but subtle flaw in our design through an X-ray cocrystal structure of the truncated derivative **5** (Figure 3b). We had assumed that the benzothiophene in **5** would bind to p38 close to its ground-state *s-trans* conformer, with the sulfur on the same side as the N–H of the adjacent amide, as opposed to the energetically less-favored *s-cis* conformation that could create lone pair/lone

^a Abbreviations: T_m , thermal denaturation assay; HuWB, human whole blood assay.

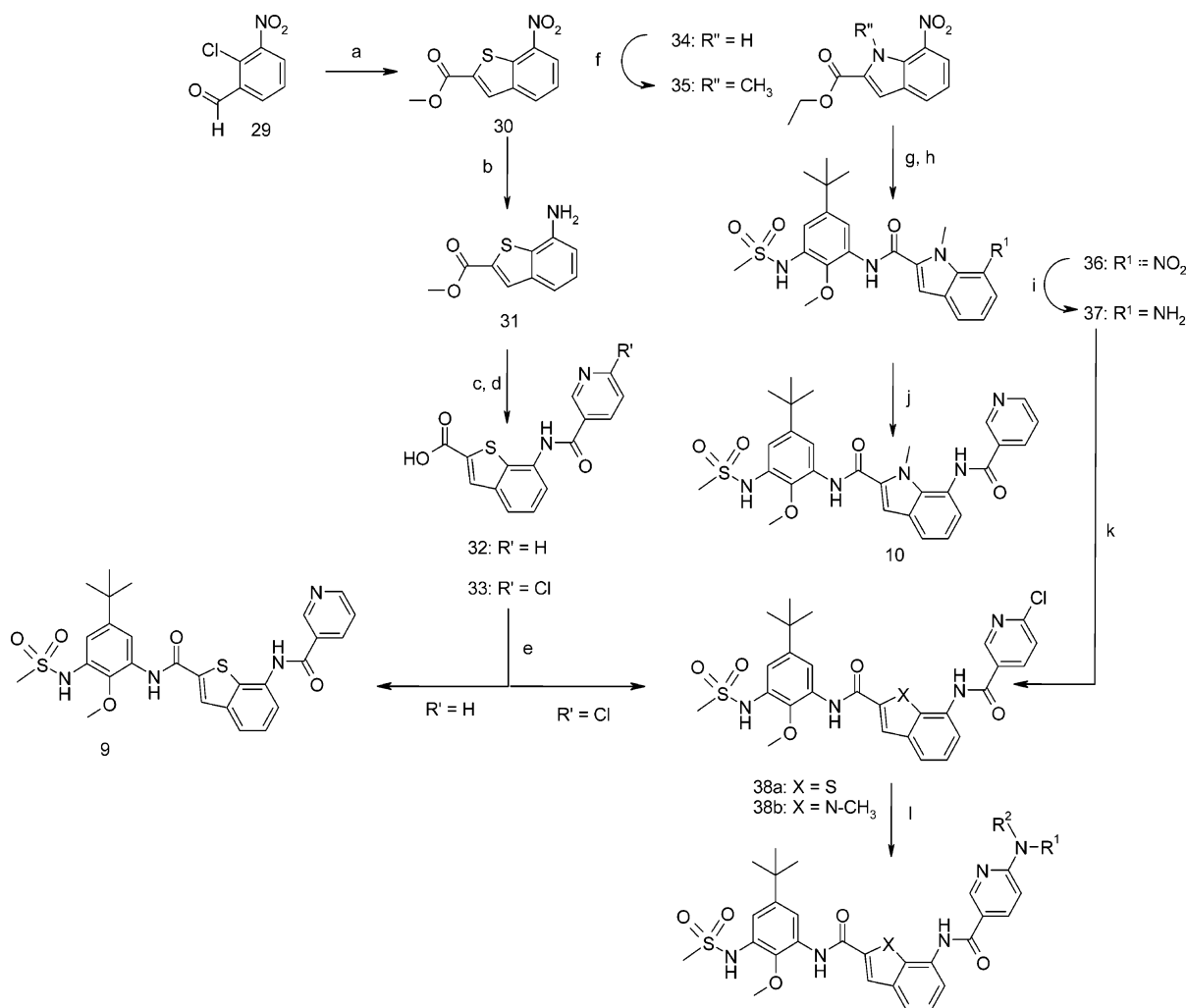
Scheme 2^a

Table 2 & 3
 11, 12, 14, 15, 17, 19, 21, 23 X = S
 13, 16, 18, 20, 22, 24 X = N-CH₃

^a Reagents and conditions: (a) K₂CO₃, methyl thioglycolate, DMF; (b) H₂, 10% Pd/C, EtOAc; (c) nicotinic acid or 6-chloronicotinic acid, Et₃N, BopCl, CH₂Cl₂; (d) LiOH, H₂O, THF; (e) **25**, HATU, HOBT, DIPEA, DMF; (f) NaH, MeI, THF; (g) NaOH, EtOH; (h) **25**, EDC, HOBT, DMF; (i) H₂, 10% Pd/C, EtOAc; (j) nicotinic acid, HOBT, EDC, DMF; (k) 6-chloronicotinic acid, HOBT, EDC, DMF; (l) HNR¹R², Δ.

pair repulsive interactions between the sulfur atom and the carbonyl oxygen. However, the X-ray cocrystal structure of compound **5** showed the benzothioephene in the *s-cis* conformation. Presumably, preference for the *s-cis* conformation in the bound state is due to repulsive interactions in the *s-trans* conformation between the carboxyl group of Glu71 and the lone pairs of the benzothioephene sulfur. Importantly, we now realized that our initial design did not optimally position the pyridyl carboxamide attachment. Based on the observed binding conformation of the benzothioephene of compound **5**, the 7-position of the benzothioephene (compound **9**) would be the better site for attaching the pyridyl carboxamide than the 4-position in our originally designed compound **8**.

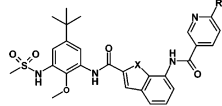
We were delighted and somewhat surprised that repositioning the pyridyl carboxamide attachment from the 4-position to the 7-position of the benzothioephene (compound **9**) resulted in a thermal denaturation temperature with p38 of 59.5 °C (IC₅₀ ≈ 1 nM). This corresponds to a greater than 2 order of magnitude (8.3 °C) increase in potency compared to the unsubstituted derivative **5**. The magnitude of this increase was initially surprising considering that addition of the ethoxymorpholino moiety (compound **1**) to the unsubstituted naphthyl urea derivative **2** provided only a 3.7 °C increase in thermal

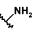
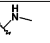
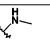
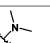
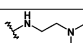
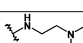
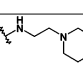
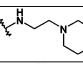
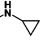
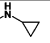


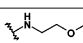
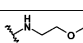
denaturation temperature. Thus, while the benzothioephene amide template appeared to be inferior to the naphthyl urea template, the pyridyl carboxamide attachment appears to compensate for this deficit so that compound **9** ends up with nearly identical potency to inhibitor **1**.

A subsequent X-ray structure of **9** provides a possible explanation for this unexpected gain in molecular potency (Figure 4). In addition to the hydrogen bonds with Met109, Glu71, and Asp168, a number of new hydrogen bonding interactions were also observed. The 7-nicotinamide N-H forms a hydrogen bond with Thr106 (the gatekeeper residue^{7a}), while the carbonyl oxygen of the 7-nicotinamide interacts with both Tyr35 and Lys53 through a water-mediated bridge.¹⁷ In addition, Tyr35 also forms a π -stacking interaction with the pyridine group of the nicotinamide.

Given the information gained through the crystal structure of **9**, we were curious why compound **8** was less potent than even the truncated benzothioephene given it still has the ability to interact with Met109 albeit in an energetically less-favored conformation. A cocrystal structure of **8** demonstrated that unlike **9**, where the benzothioephene is nearly coplanar to the adjacent

Table 2. 6-Amino Substituted Nicotinamides



Compound	X	R	T _m (°C) ^a	Inhibition of TNF α from HuWB (nM) ^c
9	S	H	59.5	1,100
10	N-CH ₃	H	57.5	3,600
11	S		61.3	430
12	S		57.7	1,100
13	N-CH ₃		61.0	500
14	S		52.4 ^b	2,200
15	S		60.3	650
16	N-CH ₃		59.6	700
17	S		62.4	550
18	N-CH ₃		61.8	250
19	S		63.9	180
20	N-CH ₃		63.6	140
21	S		63.5	670
22	N-CH ₃		63.4	150
23	S		62.3	130
24	N-CH ₃		62.8	160

^a Values are the mean of \geq two experiments, standard deviation 0.1–0.5 °C unless otherwise noted. ^b Value $n = 1$. ^c Values are the geometric means from 8 to 12 donor experiments, standard deviation typically $\pm 50\%$ of reported value.

amide carbonyl, the benzothiothiazine in compound **8** is twisted by 30°, presumably to reduce lone pair–lone pair interactions between Glu71 and the sulfur atom. The twist causes a loss in all of the productive hydrogen bonding interactions within the adenine site (Figure 5).

In addition to the benzothiothiazine, the corresponding *N*-methyl indole analogue **10** also demonstrated a similar binding potency to **9** (Table 2). While compounds **9** and **10** represented a new class of potent p38 inhibitors compared to **1**, we felt that these two inhibitors did not possess the level of in vitro potency desired in a backup compound. We felt the adenine binding site was a logical area to further explore, given that a number of p38 inhibitors gain additional binding interactions in this region.¹⁸

From the X-ray structure of **9**, it appeared possible that the inhibitor could interact not only with the N–H of Met109, but also with the adjacent carbonyl by incorporating a hydrogen bond donating group at the 6-position of the pyridine ring. To test this hypothesis, we appended a variety of amine groups to this position of the pyridine. In support of our hypothesis, we found that **11** led to an improvement in molecular potency, while

14 lost potency. In addition, inhibition of LPS-induced TNF α in human whole blood also improves as compared to **1** (Table 2; **11–13** and **15–24**). A cocrystal structure of **19** confirmed the new interaction of the N–H and the carbonyl of Met109 (Figure 6). In general, we found that small alkyl or alkoxy substituted amines (**19–24**) provided us with the best combination of in vitro potency (vide infra), likely due to increased hydrophobic interactions in this region of p38 in addition to the extra H-bonding interaction.

Given that we know that **1** can inhibit other kinases,¹⁹ compound **19** as a representative example from this new class of molecules is reasonably selective. While potent against both Lyn (230 nM) and Jnk2 (16 nM), compound **19** shows negligible inhibition of the following kinases when tested at 3 μ M: MKK1, JNK1, MAPKAP-K1a, MAPKAP-K2, MSK1, PRAK, PKA, PKCa, PDK1, PKB δ PH, SGK, S6K1, GSK3b, ROCK-II, AMPK, CHK1, CK2, PHOS. KINASE, CDK2/cyclin A, CK1, DYRK1A, PP2A, and NEK6 and the following tested at 10 μ M: Btk, Eck, EGFR, FGFR3, Hek, HGFR, IGF1R, IR, Itk, JAK3, PDGFRa, Syk, TrkA, TXK, VEGFR1.

Mouse In Vivo and Rat Pharmacokinetic Studies. To assess the potency of these new p38 inhibitors in vivo, we utilized a mouse (oral) model of LPS-stimulated TNF α production. In this model, compounds were dosed 30 min prior to LPS challenge, and plasma TNF α levels were determined 1 h later. While compounds **9** and **10** demonstrated identical in vivo efficacy to **1** in this model at a dose of 10 mg/kg, the more potent derivatives **19** and **20** also proved significantly more potent in vivo, inhibiting TNF α at a dose at or below 3 mg/kg (Table 3).

Subsequent pharmacokinetic analysis of compounds **9**, **10**, **19**, and **20** demonstrate good oral exposure and bioavailability at a dose of 10 mg/kg. Compound **20** has a comparable pharmacokinetic profile to **1**, while having an improved in vitro/in vivo potency profile (Table 4).

Conclusion

A new series of potent Phe out p38 inhibitors have been discovered through a combination of computer-assisted drug design, X-ray crystallography, and chemical intuition. Critical to the discovery of this series of inhibitors was the iterative nature of the design process based on obtaining timely structural information throughout the discovery and optimization process. This process successfully culminated in the identification of compounds with improved cellular and in vivo potency profiles to our previous clinical candidate **1**.

Experimental Section

General Methods. ¹H NMR spectra were recorded on a Bruker UltraShield-400 MHz spectrometer operating at 400 MHz in solvents, as noted. Proton coupling constants (*J* values) are rounded to the nearest Hz. All solvents were HPLC grade or better. The reactions were followed by TLC on precoated Uniplat silica gel plates purchased from Analtech. The developed plates were visualized using 254 nm UV illumination or by PMA stain. Flash column chromatography on silica gel was performed on Redi Sep prepacked disposable silica gel columns using an Isco Combiflash. Reactions were carried out under an atmosphere of N₂ at room temperature, unless otherwise noted. Purity was evaluated by analytical HPLC using a Varian Dynamax SD-200 pump coupled to a Varian Dynamax UV-1 detector (system A), or a HP 110 Agilent LCMS using a Quaternary G1311A pump coupled to a Micromass Platform LCZ detector (system B). In system A, the solvents were the following: (A) water + 0.05% TFA and (B) acetonitrile + 0.05% TFA, flow 1.2 mL/min. Column Vydac RP-18, 5 m, 250 \times 4.6 mm, Photodiode Array Detector at 220 nm;

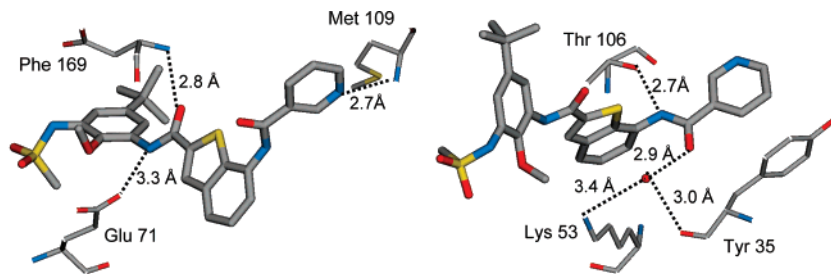


Figure 4. Two views of the cocrystal structure of 9.

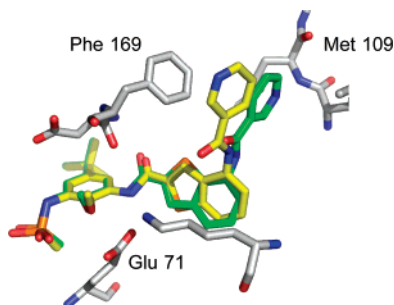


Figure 5. Cocrystal structure of 9 (green) overlaid with 8 (yellow).

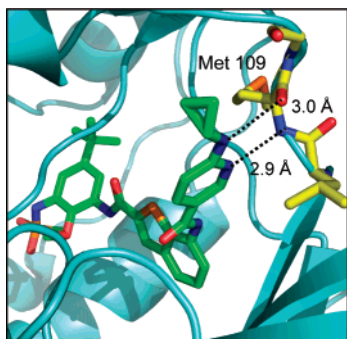


Figure 6. Cocrystal structure of 19.

Table 3. In Vivo Studies in LPS-Stimulated Mouse Proof of Principle Model

cmpd	T_m^a (°C)	inhibition of TNF α from HuWB ^b (nM)	inhibition of TNF α from LPS-treated mice at dose (mg/kg)
1	63.0	780	60% at 10
9	59.5	1100	60% at 10
10	57.5	3600	60% at 10
19	63.9	180	98% at 10; 80% at 3
20	63.6	140	75% at 10; 60% at 3

^a Values are the mean of \geq two experiments, standard deviation 0.1–0.5 °C unless otherwise noted. ^b Values are the geometric means from 8 to 12 donor experiments, standard deviation typically \pm 50% of reported value.

Table 4. Sprague–Dawley Rat Pharmacokinetics^a

cmpd	1	9	10	19	20
iv Cl (mL/min/kg)	1.7	19	3	4	5
PO C_{max} (ng/mL)	10 900	5200	9000	2400	14 000
F (%)	76	57	90	51	51

^a 1 mg/kg i.v.; 10 mg/kg p.o.

from 95% to 20% solvent (A) over 25 min. In system B, the solvents were the following: (A) water + 0.1% formic acid and (B) acetonitrile + 0.1% formic, flow 1.5 mL/min. Column Waters Sunfire C-18 Column, 4.6 \times 30 mm, 3.5 μ m, Photodiode Array Detector at 200 or 600 nm; from 95% to 5% solvent (A) over 10 min. Elemental analyses were performed by Quantitative Technologies, Whitehouse, NJ.

***N*-(3-Amino-5-*tert*-butyl-2-methoxy-phenyl)-methanesulfonamide (25):** A total of 210 g (0.82 mole) of 5-*tert*-butyl-2-methoxy-1,3-dinitro-benzene was dissolved in ethyl acetate (1 L) in a stainless steel autoclave. The autoclave was then purged with H₂ and pressured to 40 psi with vigorous stirring. The pressure was maintained at 40 psi for 4 h, the autoclave was then vented, and the reaction mixture was filtered through Celite, dried (MgSO₄), and concentrated in vacuo (151 g, 96%). The corresponding diamine (147 g, 0.76 mole) was dissolved in MTBE (1.5 L), and Hüning's base (198 mL, 1.14 mole) was added, followed by the dropwise addition of methanesulfonyl chloride (58.6 mL, 0.76 mole) over 20 min. The resulting mixture was stirred at room temperature for 2 h, quenched with 1 M NaOH (1.5 L), and stirring was continued for 10 min until the final pH = 12. The reaction mixture was extracted with 1 M NaOH, and the combined aqueous fractions were then extracted with CH₂Cl₂. Concentrated HCl (175 mL) was slowly added with vigorous stirring until the pH = 1. The organic fraction was then washed with water and concentrated in vacuo. The resulting oil was dissolved in ethyl acetate and cooled to 0 °C, after which time HCl (4 M in 1,4-dioxane) was added. The solution was stirred vigorously for 2 h, over which time the product precipitated and was collected by filtration to provide a white solid (127 g, 54%). ¹H NMR (DMSO-*d*₆, 400 MHz): δ 1.2 (s, 9H), 3.0 (s, 3H), 3.6 (s, 3H), 4.9 (br s, 2H), 6.6 (s, 2H), 8.7 (s, 1H). ESMS m/z = 272 [M + H]⁺. HPLC purity: system B, t_R 3.09 min (99%).

***N*-(5-*tert*-Butyl-2-methoxy-3-[3-[4-(2-morpholin-4-yl-ethoxy)-naphthalen-1-yl]-ureido]-phenyl)-methanesulfonamide (2):** 4-(2-Morpholin-4-yl-ethoxy)-naphthalen-1-ylamine (180 mg, 0.7 mmol) was dissolved in 1:1 CH₂Cl₂/saturated aqueous NaHCO₃ (40 mL). Phosgene (0.9 mL, 20% solution in toluene, 1.6 mmol) was then added, and the reaction was stirred vigorously for 20 min. The reaction was extracted with CH₂Cl₂, and the organic fraction was dried (MgSO₄), filtered, and concentrated in vacuo. The crude isocyanate was then dissolved in THF (10 mL), added to a solution of 25 in THF (5 mL), and the reaction mixture was then stirred for 6 h. The reaction was concentrated in vacuo and the residue was triturated with ether to afford the title compound as a white solid (150 mg, 40%). ¹H NMR (DMSO-*d*₆, 400 MHz): δ 1.2 (s, 9H), 2.4 (br s, 2H), 2.8 (br s, 2H), 3.1 (s, 3H), 3.3 (s, 2H), 3.6 (br s, 4H), 3.8 (s, 3H), 4.2 (br s, 2H), 7.0 (br s, 2H), 7.5–7.6 (m, 2H), 7.7 (d, 1H, J = 2 Hz), 8.1 (d, 1H, J = 2 Hz), 8.2 (br s, 1H), 8.3 (d, 1H, J = 2 Hz), 8.6 (s, 1H), 9.0 (s, 1H), 9.1 (s, 1H). ESMS m/z = 571 [M + H]⁺. HPLC purity: system B, t_R 2.66 min (99%).

***N*-[5-*tert*-Butyl-2-methoxy-3-(3-naphthalen-1-yl-ureido)-phenyl]-methanesulfonamide (3):** To a solution of 25 (100 mg, 0.36 mmol) in THF (1 mL) was added 1-isocyanato-naphthalene (62 mg, 0.36 mmol). The reaction mixture was stirred for 12 h and then concentrated in vacuo. Triturating with ethyl acetate afforded the title compound as an off-white solid (150 mg, 95%). ¹H NMR (DMSO-*d*₆, 400 MHz): δ 1.2 (s, 9H), 3.1 (s, 3H), 3.6 (s, 3H), 6.9 (d, 1H, J = 2 Hz), 7.4 (t, 1H, J = 2 Hz), 7.5–7.7 (m, 4H), 7.9 (d, 1H, J = 2 Hz), 8.1 (d, 1H, J = 2 Hz), 8.2–8.3 (m, 1H), 8.9 (s, 1H), 9.1 (s, 1H), 9.3 (s, 1H). HPLC purity: system B, t_R 5.31 min (98%).

Benzofuran-2-carboxylic Acid (5-*tert*-Butyl-3-methanesulfonylamino-2-methoxy-phenyl)-amide (4): Benzofuran-2-carboxylic acid (60 mg, 0.37 mmol) was suspended in DMF (2 mL). Diisopropylethylamine (40 mg, 70 μ L, 0.40 mmol) followed by

TBTU (128 mg, 0.40 mmol) and **25** (100 mg, 0.37 mmol) were then added. The resulting suspension was stirred for 15 h and then extracted with ethyl acetate. The organic fraction was washed with water and brine, dried (MgSO₄), filtered, and concentrated in vacuo. Flash column chromatography on silica gel (2:1 hexanes/ethyl acetate) afforded the title compound as a pale yellow solid (59 mg, 39%). ¹H NMR (DMSO-*d*₆, 400 MHz): δ 1.3 (s, 9H), 3.0 (s, 3H), 3.8 (s, 3H), 7.3 (d, 1H, *J* = 2 Hz), 7.4 (t, 1H, *J* = 8 Hz), 7.5 (t, 1H, *J* = 8 Hz), 7.6 (d, 1H, *J* = 2 Hz), 7.7 (d, 1H, *J* = 8 Hz), 7.8 (s, 1H), 7.9 (d, 1H, *J* = 8 Hz), 9.2 (s, 1H), 9.9 (s, 1H). ESMS *m/z* = 417 [M + H]⁺. HPLC purity: system B, *t*_R 5.31 min (99%). Anal. Calcd for C₂₁H₂₄N₂O₅S·0.25 H₂O: C, 59.91; H, 5.87; N, 6.65. Found: C, 60.85; H, 5.95; N, 6.30.

Benzo[*b*]thiophene-2-carboxylic Acid (5-*tert*-Butyl-3-methanesulfonylamino-2-methoxy-phenyl)-amide (5): Compound **5** was prepared as described above from benzo[*b*]thiophene-2-carboxylic acid to afford the title compound as a pale yellow solid (50 mg, 16%). ¹H NMR (DMSO-*d*₆, 400 MHz): δ 1.2 (s, 9H), 3.0 (s, 3H), 3.7 (s, 3H), 7.2 (d, 1H, *J* = 2 Hz), 7.5–7.6 (m, 3H), 8.0 (d, 1H, *J* = 7 Hz), 8.1 (d, 1H, *J* = 7 Hz), 8.3 (s, 1H), 9.2 (s, 1H), 10.1 (s, 1H). ESMS *m/z* = 433 [M + H]⁺. HPLC purity: system B, *t*_R 5.46 min (99%). Anal. Calcd for C₂₁H₂₄N₂O₄S₂·0.5H₂O: C, 57.12; H, 5.71; N, 6.34. Found: C, 56.96; H, 5.47; N, 6.19.

1*H*-Indole-2-carboxylic Acid (5-*tert*-Butyl-3-methanesulfonylamino-2-methoxy-phenyl)-amide (6): Compound **6** was prepared as described above from indole-2-carboxylic acid to afford the title compound as a beige solid (9 mg, 6%). ¹H NMR (DMSO-*d*₆, 400 MHz): δ 1.2 (s, 9H), 3.0 (s, 3H), 3.7 (s, 3H), 7.0 (t, 1H, *J* = 8 Hz), 7.1–7.2 (m, 2H), 7.3 (s, 1H), 7.4 (d, 1H, *J* = 8 Hz), 7.5 (s, 1H), 7.6 (d, 1H, *J* = 8 Hz), 9.1 (s, 1H), 9.7 (s, 1H), 11.7 (s, 1H). ESMS *m/z* = 414 [M – H][–].

1-Methyl-1*H*-indole-2-carboxylic Acid (5-*tert*-Butyl-3-methanesulfonylamino-2-methoxy-phenyl)-amide (7): Compound **7** was prepared as described above to afford the title compound as a white solid (50 mg, 20%). ¹H NMR (DMSO-*d*₆, 400 MHz): δ 1.3 (s, 9H), 3.1 (s, 3H), 3.8 (s, 3H), 4.0 (s, 3H), 7.1 (t, 1H, *J* = 8 Hz), 7.2 (d, 1H, *J* = 2 Hz), 7.3–7.4 (m, 2H), 7.5 (d, 1H, *J* = 2 Hz), 7.6 (d, 1H, *J* = 8 Hz), 7.7 (d, 1H, *J* = 8 Hz), 9.2 (s, 1H), 9.8 (s, 1H). ESMS *m/z* = 430 [M + H]⁺.

4-Nitro-benzo[*b*]thiophene-2-carboxylic Acid (5-*tert*-Butyl-3-methanesulfonylamino-2-methoxy-phenyl)-amide (27): 4-Nitrobenzo[*b*]thiophene-2-carboxylic acid (60 mg, 0.27 mmol) was suspended in DMF (2 mL). Diisopropylethylamine (40 mg, 70 μL, 0.40 mmol) followed by TBTU (128 mg, 0.40 mmol) and **25** (100 mg, 0.37 mmol) was then added. The resulting suspension was stirred for 15 h and then extracted with ethyl acetate. The organic fraction was washed with water and brine, dried (MgSO₄), filtered, and concentrated in vacuo. Flash column chromatography on silica gel (2:1 hexanes/ethyl acetate) afforded the title compound as a pale yellow solid (59 mg, 39%). ¹H NMR (DMSO-*d*₆, 400 MHz): δ 1.2 (s, 9H), 3.0 (s, 3H), 3.7 (s, 3H), 7.3 (d, 1H, *J* = 2 Hz), 7.4 (d, 1H, *J* = 2 Hz), 7.7 (t, 1H, *J* = 8 Hz), 8.4 (d, 1H, *J* = 8 Hz), 8.5 (d, 1H, *J* = 8 Hz), 9.1 (s, 1H), 9.2 (s, 1H), 10.7 (s, 1H). ESMS *m/z* = 476 [M – H][–].

4-Amino-benzo[*b*]thiophene-2-carboxylic Acid (5-*tert*-Butyl-3-methanesulfonylamino-2-methoxy-phenyl)-amide (28): A mixture of **27** (200 mg, 0.42 mmol) and 10% Pd/C (50 mg) was suspended in ethyl acetate (2 mL). The reaction was placed under 1 atm of H₂ (balloon). The black suspension was stirred for 12 h then filtered through Celite and washed with ethyl acetate until the filtrate was clear and colorless. The filtrate was dried (MgSO₄) and concentrated in vacuo to afford the title compound as a pale yellow solid (170 mg, 90%). ¹H NMR (DMSO-*d*₆, 400 MHz): δ 1.2 (s, 9H), 3.0 (s, 3H), 3.7 (s, 3H), 5.8 (br s, 2H), 6.5 (d, 1H, *J* = 8 Hz), 7.1–7.2 (m, 2H), 7.3 (d, 1H, *J* = 2 Hz), 7.7 (d, 1H, *J* = 2 Hz), 8.5 (s, 1H), 9.1 (br s, 1H), 9.5 (s, 1H). ESMS *m/z* = 448 [M + H]⁺.

***N*-[2-(5-*tert*-Butyl-3-methanesulfonylamino-2-methoxy-phenyl)carbamoyl]-benzo[*b*]thiophen-4-yl]-nicotinamide (8):** Nicotinic acid (19 mg, 0.11 mmol) and **28** (50 mg, 0.1 mmol) were dissolved in DMF (2 mL). EDC (21 mg, 0.11 mmol) and HOBt (15 mg, 0.1 mmol) were then added, and the brown solution was

stirred for 72 h. The reaction was extracted with ethyl acetate, and the organic fraction was washed with water and brine, dried (MgSO₄), filtered, and concentrated in vacuo. Flash column chromatography on silica gel (100% ethyl acetate) afforded the title compound as a pale yellow solid (22 mg, 36%). ¹H NMR (DMSO-*d*₆, 400 MHz): δ 1.1 (s, 9H), 2.9 (s, 3H), 3.5 (s, 3H), 7.1 (d, 1H, *J* = 2 Hz), 7.2 (d, 1H, *J* = 2 Hz), 7.4 (d, 1H, *J* = 8 Hz), 7.5–7.6 (m, 2H), 7.8 (d, 1H, *J* = 8 Hz), 8.2 (d, 1H, *J* = 8 Hz), 8.3 (s, 1H), 8.6 (d, 1H, *J* = 8 Hz), 9.0 (s, 1H), 9.1 (s, 1H), 10.0 (s, 1H), 10.6 (s, 1H). ESMS *m/z* = 553 [M + H]⁺.

7-Nitro-benzo[*b*]thiophene-2-carboxylic Acid Methyl Ester (30): Compound **29** (11 g, 60 mmol) was dissolved in DMF (100 mL) and cooled to 0 °C. To this solution was added K₂CO₃ (9.1 g, 66 mmol) followed by methyl thioglycolate (6.4 g, 61 mmol), and the reaction was warmed to room temperature. The reaction mixture was stirred for 12 h, after which time a solid precipitate had formed. Water was added to provide a homogeneous solution, and the reaction mixture was cooled to 0 °C to precipitate the desired product. The solid was filtered and washed with water until the filtrate was clear and colorless, providing the title compound as a white solid (13.3 g, 94%). ¹H NMR (DMSO-*d*₆, 400 MHz): δ 3.9 (s, 3H), 7.8 (t, 1H, *J* = 8 Hz), 8.4 (s, 1H), 8.5 (d, 1H, *J* = 8 Hz), 8.6 (d, 1H, *J* = 8 Hz), ESMS *m/z* = 238 [M + H]⁺.

7-Amino-benzo[*b*]thiophene-2-carboxylic Acid Methyl Ester (31): A mixture of **30** (1.0 g, 4.2 mmol) and 10% Pd/C (400 mg) was suspended in ethyl acetate (40 mL). The reaction was placed under 1 atm of H₂ (balloon). The black suspension was stirred for 12 h, then filtered through Celite, and washed with ethyl acetate until the filtrate was clear and colorless. The filtrate was dried (MgSO₄), filtered, and then concentrated in vacuo to afford the title compound as a yellow solid (860 mg, 98%). ¹H NMR (DMSO-*d*₆, 400 MHz): δ 3.9 (s, 3H), 5.6 (s, 2H), 6.7 (d, 1H, *J* = 8 Hz), 7.1 (t, 1H, *J* = 8 Hz), 7.2 (d, 1H, *J* = 8 Hz), 8.0 (s, 1H). ESMS *m/z* = 207 [M + H]⁺.

7-[(Pyridine-3-carbonyl)-amino]-benzo[*b*]thiophene-2-carboxylic Acid (32): Nicotinic acid (400 mg, 3.3 mmol) was suspended in CH₂Cl₂ (20 mL). Triethylamine (330 mg, 3.3 mmol, 445 μL) followed by BopCl (830 mg, 3.3 mmol) was then added, and the suspension was stirred for 15 min. A solution of **31** (450 mg, 2.2 mmol) in CH₂Cl₂ (2 mL) was added, and the reaction mixture was stirred for 12 h. The reaction was concentrated in vacuo and extracted with ethyl acetate. The organic fraction was washed with water and brine, dried (MgSO₄), filtered, and concentrated in vacuo to afford the corresponding amide as a yellow solid (460 mg, 68%). ¹H NMR (DMSO-*d*₆, 400 MHz): δ 3.9 (s, 3H), 7.6–7.7 (m, 3H), 7.9 (d, 1H, *J* = 8 Hz), 8.2 (s, 1H), 8.4 (d, 1H, *J* = 8 Hz), 8.8 (d, 1H, *J* = 8 Hz), 9.2 (s, 1H), 10.9 (s, 1H). ESMS *m/z* = 313 [M + H]⁺.

The above amide was suspended in THF (25 mL) and water (8 mL) and LiOH·H₂O (200 mg, 4.9 mmol) was added. The reaction mixture was stirred for 24 h. The solvent was removed in vacuo and extracted with ethyl acetate. The aqueous fraction was acidified with 1 M HCl to precipitate the product, which was then collected by filtration to provide a white solid (390 mg, 54%). ¹H NMR (DMSO-*d*₆, 400 MHz): δ 7.6–7.7 (m, 3H), 7.9 (d, 1H, *J* = 8 Hz), 8.1 (s, 1H), 8.4 (d, 1H, *J* = 8 Hz), 8.8 (d, 1H, *J* = 8 Hz), 9.2 (s, 1H), 10.8 (s, 1H), 13.5 (s, 1H). ESMS *m/z* = 299 [M + H]⁺.

7-[(6-Chloro-pyridine-3-carbonyl)-amino]-benzo[*b*]thiophene-2-carboxylic Acid (33): To a solution of 6-chloronicotinic acid (490 mg, 3.1 mmol) and triethylamine (800 μL, 5.9 mmol) in CH₂Cl₂ (20 mL) was added BopCl (1.5 g, 5.9 mmol). After 15 min, a solution of **31** (540 mg, 2.6 mmol) in CH₂Cl₂ (10 mL) was added. The reaction was stirred for 12 h and then extracted with ethyl acetate. The organic fraction was washed with saturated aqueous NaHCO₃, water, and brine, dried (MgSO₄), filtered, and concentrated in vacuo. Flash column chromatography on silica gel (4:1 hexanes/ethyl acetate) provided the corresponding amide as a light yellow solid (613 mg, 68%). ¹H NMR (DMSO-*d*₆, 400 MHz): δ 3.9 (s, 3H), 7.6–7.5 (m, 2H), 7.8 (d, 1H, *J* = 8 Hz), 7.9 (dd, 1H, *J* = 8.0, 2 Hz), 8.3 (s, 1H), 8.4 (dd, 1H, *J* = 8, 2 Hz), 9.0 (d, 1H, *J* = 2 Hz), 10.9 (s, 1H).

The above amide (91 mg, 0.26 mmol) was dissolved in 1:1 THF/MeOH (6 mL) and 1 N NaOH (660 μ L, 0.66 mmol) was then added. The solution was stirred for 12 h and then extracted with CH_2Cl_2 . The aqueous fraction was acidified with 1 N HCl until the pH = 4 and then extracted with CH_2Cl_2 . The organic fraction was washed with water and brine, dried (MgSO_4), filtered, and concentrated in vacuo to provide the title compound as a light yellow solid (90 mg, 100%). ^1H NMR ($\text{DMSO}-d_6$, 400 MHz): δ 7.5–7.6 (m, 2H), 7.8 (d, 1H, $J = 8$ Hz), 7.9 (d, 1H, $J = 8$ Hz), 8.2 (s, 1H), 8.4 (d, 1H, $J = 2$ Hz), 9.0 (d, 1H, $J = 2$ Hz), 10.9 (s, 1H).

***N*-[2-(5-*tert*-Butyl-3-methanesulfonylamino-2-methoxy-phenyl-carbamoyl)-benzo[*b*]thiophen-7-yl]-nicotinamide (9):** Compound **32** (20 g, 67 mmol) and **25** (18.6 g, 67 mmol) were suspended in DMF (450 mL), and diisopropylethylamine (17 g, 23 mL, 134 mmol) was then added. The reaction mixture was stirred for 20 min, then HATU (30.6 g, 80.5 mmol) and HOBT (10.9 g, 80.5 mmol) were added. The solution was stirred for an additional 2 days. After 2 d, the reaction was poured into water and the aqueous portion was decanted, and the resultant brown residue was suspended in CH_2Cl_2 to afford a yellow suspension that was then filtered through Celite. The filtrate was dried (MgSO_4), filtered, and concentrated in vacuo to afford the title compound as a yellow solid (27 g, 73%). ^1H NMR ($\text{DMSO}-d_6$, 400 MHz): δ 1.3 (s, 9H), 3.1 (s, 3H), 3.7 (s, 3H), 7.3 (d, 1H, $J = 2$ Hz), 7.4 (d, 1H, $J = 2$ Hz), 7.5–7.6 (m, 2H), 7.7 (dd, 1H, $J = 7, 2$ Hz), 7.9 (dd, 1H, $J = 7, 2$ Hz), 8.4 (dt, 1H, $J = 6, 2$ Hz), 8.4 (s, 1H), 8.8 (dd, 1H, $J = 6, 2$ Hz), 9.2 (d, 1H, $J = 2$ Hz), 9.2 (s, 1H), 10.2 (s, 1H), 10.9 (s, 1H). ESMS $m/z = 553$ [$\text{M} + \text{H}$] $^+$.

7-Nitroindole-2-carboxylic Acid (5-*tert*-Butyl-3-methanesulfonylamino-2-methoxy-phenyl)-amide (36): To a suspension of NaH (60% w/w in mineral oil, 0.3 g, 6.41 mmol) in DMF (20 mL) was added ethyl 7-nitroindole-2-carboxylate (1.5 g, 6.4 mmol). The reaction mixture was stirred for 1 h and then MeI (0.8 mL, 13.0 mmol) in DMF (4 mL) was added dropwise. After 5.5 h, the reaction mixture was poured onto ice and extracted with ethyl acetate. The organic fraction was washed with water and brine, dried (MgSO_4), filtered, and concentrated in vacuo. Flash column chromatography on silica gel provides **35** as an off-white solid (800 mg, 50%). ^1H NMR ($\text{DMSO}-d_6$, 400 MHz): δ 1.5 (t, 3H, $J = 2$ Hz), 4.0 (s, 3H), 4.4 (q, 2H, $J = 2$ Hz), 7.1 (t, 1H, $J = 2$ Hz), 7.4 (s, 1H), 7.8 (d, 1H, $J = 2$ Hz), 7.9 (dd, 2H, $J = 8, 2$ Hz).

The above ester (0.54 g) was dissolved in EtOH (15 mL) and 2 N aqueous NaOH (5 mL) and heated to reflux for 2.5 h. The reaction was then cooled to room temperature and stirred for an additional 12 h. The ethanol was removed in vacuo, and the residue was acidified with 2 N HCl. A white precipitate formed, was collected by filtration, washed with water, and dried in vacuo. Recrystallization from 2-propanol provided the corresponding carboxylic acid as a white solid (250 mg, 52%). ^1H NMR ($\text{DMSO}-d_6$, 400 MHz): δ 3.8 (s, 3H), 7.3 (t, 1H, $J = 2$ Hz), 7.4 (s, 1H), 7.8 (d, 1H, $J = 2$ Hz), 8.1 (d, 1H, $J = 2$ Hz), 13.1 (br s, 1H).

The above acid (1.0 g, 4.9 mmol), **25** (1.3 g, 4.9 mmol), HOBT (655 mg, 4.9 mmol), and EDC (930 mg, 4.9 mmol) were dissolved in DMF (25 mL) and stirred for 12 h. The reaction mixture was then extracted with ethyl acetate. The organic fraction was washed with saturated aqueous NH_4Cl , water, and brine, dried (MgSO_4), filtered, and concentrated in vacuo. Flash column chromatography on silica gel (4:1 hexanes/ethyl acetate) afforded the title compound as a white solid (700 mg, 31%). ^1H NMR ($\text{DMSO}-d_6$, 400 MHz): δ 1.3 (s, 9H), 3.1 (s, 3H), 3.7 (s, 3H), 3.9 (s, 3H), 7.3 (d, 1H, $J = 2$ Hz), 7.4 (t, 1H, $J = 8$ Hz), 7.6–7.7 (m, 2H), 8.3 (m, 2H), 9.3 (s, 1H), 11.8 (s, 1H). ESMS $m/z = 461$ [$\text{M} + \text{H}$] $^+$.

7-Aminoindole-2-carboxylic Acid (5-*tert*-Butyl-3-methanesulfonylamino-2-methoxy-phenyl)-amide (37): A mixture of **36** (60 mg, 0.13 mmol) and 10% Pd/C (20 mg) were suspended in ethyl acetate (2 mL). The reaction was placed under 1 atm of H_2 (balloon). The black suspension was stirred for 12 h then filtered through Celite and washed with ethyl acetate until the filtrate was clear and colorless. Concentration in vacuo followed by triturating with 1:1 CH_2Cl_2 /ether afforded the title compound as an off-white solid (55 mg, 98%). ^1H NMR ($\text{DMSO}-d_6$, 400 MHz): δ 1.3 (s,

9H), 3.0 (s, 3H), 3.7 (s, 3H), 3.9 (s, 3H), 5.4 (s, 2H), 6.4 (d, 1H, $J = 8$ Hz), 6.9–7.0 (m, 2H), 7.3 (d, 1H, $J = 2$ Hz), 7.4 (d, 1H, $J = 2$ Hz), 7.6 (d, 1H, $J = 2$ Hz), 9.8 (s, 1H), 11.4 (s, 1H). ESMS $m/z = 431$ [$\text{M} + \text{H}$] $^+$.

***N*-[2-(5-*tert*-Butyl-3-methanesulfonylamino-2-methoxy-phenyl-carbamoyl)-1-methylindol-7-yl]-nicotinamide (10):** Compound **37** (218 mg, 0.5 mmol), nicotinic acid (74 mg, 0.6 mmol), HOBT (80 mg, 0.6 mmol), and EDC (115 mg, 0.6 mmol) were suspended in DMF (5 mL). After 12 h, additional nicotinic acid (37 mg, 0.3 mmol), HOBT (41 mg, 0.3 mmol), and EDC (58 mg, 0.3 mmol) were added, and the reaction mixture was stirred for an additional 5 h. The reaction was then extracted with ethyl acetate, and the organic fraction was washed with water and brine, dried (Na_2SO_4), filtered, and concentrated in vacuo. Preparative HPLC afforded the title compound as a white solid (160 mg, 59%). ^1H NMR ($\text{DMSO}-d_6$, 400 MHz): δ 1.2 (s, 9H), 3.0 (s, 3H), 3.7 (s, 3H), 4.0 (s, 3H), 7.0–7.1 (m, 2H), 7.2 (d, 1H, $J = 2$ Hz), 7.3 (s, 1H), 7.5 (d, 1H, $J = 2$ Hz), 7.6 (dd, 1H, $J = 8, 5$ Hz), 7.7 (dd, 1H, $J = 7, 2$ Hz), 8.4 (dd, 1H, $J = 8, 2$ Hz), 8.8 (dd, 1H, $J = 5, 2$ Hz), 9.2 (m, 2H), 9.8 (s, 1H), 10.6 (s, 1H). ESMS $m/z = 550$ [$\text{M} + \text{H}$] $^+$.

***N*-[2-(5-*tert*-Butyl-3-methanesulfonylamino-2-methoxy-phenylcarbamoyl)-benzo[*b*]thiophen-7-yl]-6-chloro-nicotinamide (38a):** To a solution of **33** (50 mg, 0.15 mmol) in DMF (1.5 mL) was added EDC (43 mg, 0.22 mmol) and HOBT (30 mg, 0.22 mmol). The reaction was stirred for 15 min, then **25** (49 mg, 0.18 mmol) was added. The reaction was stirred for 12 h, and then DMF was removed and the residue was taken up in ethyl acetate. The organic fraction was washed with water and brine, dried (MgSO_4), filtered, and concentrated in vacuo. Flash column chromatography on silica gel (5:1 hexanes/ethyl acetate) afforded the title compound as a white solid (36 mg, 41%). ^1H NMR ($\text{DMSO}-d_6$, 400 MHz): δ 1.2 (s, 9H), 3.0 (s, 3H), 3.7 (s, 3H), 7.2 (d, 1H, $J = 2$ Hz), 7.4 (d, 1H, $J = 2$ Hz), 7.5–7.6 (m, 2H), 7.7 (d, 1H, $J = 8$ Hz), 7.9 (dd, 1H, $J = 7, 2$ Hz), 8.4–8.5 (m, 2H), 9.0 (d, 1H, $J = 2$ Hz), 9.2 (s, 1H), 10.2 (s, 1H), 10.9 (s, 1H).

7-[(6-Chloro-pyridine-3-carbonyl)-amino]-1-methyl-indole-2-carboxylic Acid (5-*tert*-Butyl-3-methanesulfonylamino-2-methoxy-phenyl)-amide (38b): A mixture of **36** (310 mg, 0.7 mmol), 6-chloro nicotinic acid (170 mg, 1.1 mmol), HOBT (149 mg, 1.1 mmol), and EDC (210 mg, 1.1 mmol) were dissolved in DMF (5 mL) and stirred for 16 h. The reaction mixture was extracted with ethyl acetate, and the organic fraction was washed with water and brine, dried (Na_2SO_4), filtered, and concentrated in vacuo. Flash column chromatography on silica gel (3:1 hexanes/ethyl acetate) afforded the title compound as a yellow foam (350 mg, 86%). ^1H NMR ($\text{DMSO}-d_6$, 400 MHz): δ 1.3 (s, 9H), 3.0 (s, 3H), 3.7 (s, 3H), 4.0 (s, 3H), 7.0–7.1 (m, 2H), 7.2 (d, 1H, $J = 2$ Hz), 7.3 (s, 1H), 7.5 (d, 1H, $J = 2$ Hz), 7.7 (dd, 1H, $J = 7, 2$ Hz), 7.8 (d, 1H, $J = 8$ Hz), 8.4 (dd, 1H, $J = 8, 2$ Hz), 9.0 (d, 1H, $J = 2$ Hz), 9.2 (s, 1H), 9.9 (s, 1H), 10.6 (s, 1H). ESMS $m/z = 584$ [$\text{M} + \text{H}$] $^+$.

6-Amino-*N*-[2-(5-*tert*-butyl-3-methanesulfonylamino-2-methoxy-phenylcarbamoyl)-benzo[*b*]thiophen-7-yl]-nicotinamide (11): Compound **38a** (34 mg, 0.06 mmol) was placed in a sealed tube and 4-methoxybenzylamine (200 μ L) was added. The vessel was purged with argon and then heated to 100 $^\circ\text{C}$. After 4 h, the reaction mixture was cooled to room temperature and extracted with ethyl acetate. The organic fraction was washed with water and brine, dried (MgSO_4), filtered, and concentrated in vacuo. Flash column chromatography on silica gel (1:9 MeOH/ CH_2Cl_2) provided the corresponding benzyl amine as an off-white solid (26 mg, 65%). ^1H NMR ($\text{DMSO}-d_6$, 400 MHz): δ 1.3 (s, 9H), 3.0 (s, 3H), 3.7 (s, 6H), 4.5 (d, 2H, $J = 6$ Hz), 6.4 (d, 1H, $J = 8$ Hz), 6.8 (d, 1H, $J = 8$ Hz), 7.2–7.3 (m, 3H), 7.4 (d, 1H, $J = 2$ Hz), 7.5–7.6 (m, 2H), 7.7–7.8 (m, 3H), 7.9 (dd, 1H, $J = 6, 2$ Hz), 8.0–8.1 (m, 1H), 8.3 (s, 1H), 8.7 (d, 1H, $J = 2$ Hz), 9.2 (s, 1H), 10.1 (s, 1H), 10.2 (s, 1H). ESMS $m/z = 688$ [$\text{M} + \text{H}$] $^+$.

The above amine (94 mg, 0.1 mmol) was placed in a sealed tube and trifluoroacetic acid (800 μ L) was added. The solution was purged with argon and then heated to 75 $^\circ\text{C}$ for 12 h. The reaction was cooled to room temperature, diluted with toluene, and concentrated in vacuo. The residue was taken up in ethyl acetate

and washed with saturated aqueous NaHCO₃, water and brine, dried (MgSO₄), filtered, and concentrated in vacuo. Flash column chromatography on silica gel (1:13 MeOH/CH₂Cl₂) afforded the title compound as a white solid (54 mg, 70%). ¹H NMR (DMSO-*d*₆, 400 MHz): δ 1.3 (s, 9H), 3.0 (s, 3H), 3.7 (s, 3H), 6.5 (d, 1H, *J* = 9 Hz), 6.7 (s, 2H), 7.3 (d, 1H, *J* = 2 Hz), 7.4 (d, 1H, *J* = 2 Hz), 7.5–7.6 (m, 2H), 7.9 (d, 1H, *J* = 7 Hz), 8.0 (d, 1H, *J* = 9 Hz), 8.4 (s, 1H), 8.6 (s, 1H), 9.2 (s, 1H), 10.1 (s, 1H), 10.3 (s, 1H). HPLC purity: system A, *t*_R 8.94 min (99%). ESMS *m/z* = 568 [M + H]⁺.

***N*-[2-(5-*tert*-Butyl-3-methanesulfonylamino-2-methoxy-phenylcarbamoyl)-benzo[*b*]thiophen-7-yl]-6-methylamino-nicotinamide (12):** Prepared as described above (30%, off-white solid). ¹H NMR (DMSO-*d*₆, 400 MHz): δ 1.3 (s, 9H), 2.8 (d, 3H, *J* = 4 Hz), 3.3 (s, 3H), 3.7 (s, 3H), 6.5 (d, 1H, *J* = 8 Hz), 7.2 (s, 1H), 7.4 (s, 1H), 7.5 (d, 2H, *J* = 4 Hz), 7.8 (d, 1H, *J* = 6 Hz), 7.9 (dd, 2H, *J* = 8, 6 Hz), 8.3 (d, 1H, *J* = 6 Hz), 8.7 (s, 1H), 9.2 (s, 1H), 10.2 (s, 1H), 10.3 (s, 1H). HPLC purity: system A, *t*_R 9.03 min (99%), system B, *t*_R 2.98 min (99%). ESMS *m/z* = 582 [M + H]⁺.

1-Methyl-7-[(6-methylamino-pyridine-3-carbonyl)-amino]-indole-2-carboxylic Acid (5-*tert*-Butyl-3-methanesulfonylamino-2-methoxy-phenyl)-amide (13): Compound **13** was prepared as described above (30%, off-white solid). ¹H NMR (DMSO-*d*₆, 400 MHz): δ 1.2 (s, 9H), 2.8 (d, 3H, *J* = 5 Hz), 3.0 (s, 3H), 3.7 (s, 3H), 4.0 (s, 3H), 6.5 (d, 1H, *J* = 9 Hz), 7.0–7.1 (m, 2H), 7.2–7.3 (m, 1H), 7.4 (d, 1H, *J* = 2 Hz), 7.5 (s, 1H), 7.6 (d, 1H, *J* = 2 Hz), 7.7 (dd, 1H, *J* = 8, 2 Hz), 7.9 (d, 1H, *J* = 8 Hz), 8.7 (s, 1H), 9.1 (s, 1H), 9.8 (s, 1H), 10.0 (s, 1H). ESMS *m/z* = 579 [M + H]⁺.

***N*-[2-(5-*tert*-Butyl-3-methanesulfonylamino-2-methoxyphenylcarbamoyl)-benzo[*b*]thiophen-7-yl]-6-dimethylamino-nicotinamide (14):** Compound **14** was prepared as described above (50%, off-white solid). ¹H NMR (DMSO-*d*₆, 400 MHz): δ 1.2 (s, 9H), 3.0 (s, 3H), 3.1 (s, 6H), 3.7 (s, 3H), 6.7 (d, 1H, *J* = 9 Hz), 7.2 (d, 1H, *J* = 2 Hz), 7.4 (s, 1H), 7.5–7.6 (m, 2H), 7.8 (dd, 1H, *J* = 9, 3 Hz), 8.1 (dd, 1H, *J* = 9, 3 Hz), 8.3 (s, 1H), 8.7 (d, 1H, *J* = 2 Hz), 9.2 (s, 1H), 10.1 (s, 1H), 10.3 (s, 1H). HPLC purity: system A, *t*_R 8.94 min (97%). ESMS *m/z* = 596 [M + H]⁺.

***N*-[2-(5-*tert*-Butyl-3-methanesulfonylamino-2-methoxy-phenylcarbamoyl)-benzo[*b*]thiophen-7-yl]-6-(2-dimethylamino-ethylamino)-nicotinamide (15):** Compound **15** was prepared as described above (34%, off-white solid). ¹H NMR (DMSO-*d*₆, 400 MHz): δ 1.2 (s, 9H), 2.2 (s, 6H), 2.4–2.5 (m, 2H), 3.0 (s, 3H), 3.4–3.5 (m, 2H), 3.7 (s, 3H), 6.9 (d, 1H, *J* = 9 Hz), 7.2 (d, 1H, *J* = 2 Hz), 7.3 (d, 1H, *J* = 2 Hz), 7.4–7.5 (m, 2H), 7.8 (dd, 1H, *J* = 6.0, 2 Hz), 7.9 (dd, 1H, *J* = 9, 2 Hz), 8.3 (s, 1H), 8.7 (d, 1H, *J* = 2 Hz), 9.2 (br s, 1H), 10.1 (s, 1H), 10.2 (s, 1H). HPLC purity: system A, *t*_R 8.54 min (99%), system B, *t*_R 2.61 min (99%). ESMS *m/z* = 639 [M + H]⁺.

7-[(6-(2-Dimethylamino-ethylamino)-pyridine-3-carbonyl)-amino]-1-methyl-indole-2-carboxylic Acid (5-*tert*-Butyl-3-methanesulfonylamino-2-methoxy-phenyl)-amide (16): Compound **16** was prepared as described above (42%, off-white solid). ¹H NMR (DMSO-*d*₆, 400 MHz): δ 1.2 (s, 9H), 2.1 (s, 6H), 2.3–2.4 (m, 2H), 3.0 (s, 3H), 3.4–3.5 (m, 2H), 3.7 (s, 3H), 4.0 (s, 3H), 6.5 (d, 1H, *J* = 9 Hz), 7.0–7.1 (m, 3H), 7.2–7.3 (m, 1H), 7.4 (d, 1H, *J* = 2 Hz), 7.5 (d, 1H, *J* = 2 Hz), 7.6 (d, 1H, *J* = 7, 2 Hz), 7.9 (d, 1H, *J* = 7 Hz), 8.7 (d, 1H, *J* = 2 Hz), 9.1 (s, 1H), 9.8 (s, 1H), 10.0 (s, 1H). HPLC purity: system A, *t*_R 8.38 min (99%). ESMS *m/z* = 636 [M + H]⁺.

***N*-[2-(5-*tert*-Butyl-3-methanesulfonylamino-2-methoxy-phenylcarbamoyl)-benzo[*b*]thiophen-7-yl]-6-(2-morpholin-4-yl-ethylamino)-nicotinamide (17):** Compound **17** was prepared as described above (40%, off-white solid). ¹H NMR (DMSO-*d*₆, 400 MHz): δ 1.2 (s, 9H), 2.3–2.4 (m, 6H), 3.0 (s, 3H), 3.4–3.5 (m, 2H), 3.6–3.7 (m, 4H), 3.8 (s, 3H), 6.5 (d, 1H, *J* = 9 Hz), 7.1–7.2 (m, 1H), 7.3 (d, 1H, *J* = 2 Hz), 7.4 (d, 1H, *J* = 2 Hz), 7.5–7.6 (m, 2H), 7.8 (dd, 1H, *J* = 9, 2 Hz), 7.9 (dd, 1H, *J* = 9, 2 Hz), 8.3 (s, 1H), 8.7 (d, 1H, *J* = 2 Hz), 9.3 (br s, 1H), 10.1 (s, 1H), 10.3 (s, 1H). ESMS *m/z* = 681 [M + H]⁺.

1-Methyl-7-[(6-(2-morpholin-4-yl-ethylamino)-pyridine-3-carbonyl)-amino]-indole-2-carboxylic Acid (5-*tert*-Butyl-3-meth-

anesulfonylamino-2-methoxy-phenyl)-amide (18): Compound **18** was prepared as described above (50%, off-white solid). ¹H NMR (DMSO-*d*₆, 400 MHz): δ 1.2 (s, 9H), 2.3–2.4 (m, 6H), 3.0 (s, 3H), 3.4–3.5 (m, 2H), 3.6 (t, 4H, *J* = 4 Hz), 3.7 (s, 3H), 4.0 (s, 3H), 6.5 (d, 1H, *J* = 9 Hz), 7.0–7.1 (m, 3H), 7.2 (d, 1H, *J* = 2 Hz), 7.4 (s, 1H), 7.5 (d, 1H, *J* = 2 Hz), 7.6 (dd, 1H, *J* = 8, 2 Hz), 7.9 (d, 1H, *J* = 8 Hz), 8.7 (d, 1H, *J* = 2 Hz), 9.2 (s, 1H), 9.8 (s, 1H), 10.0 (s, 1H). HPLC purity: system A, *t*_R 9.86 min (97%). ESMS *m/z* = 678 [M + H]⁺.

***N*-[2-(5-*tert*-Butyl-3-methanesulfonylamino-2-methoxy-phenylcarbamoyl)-benzo[*b*]thiophen-7-yl]-6-cyclopropylamino-nicotinamide (19):** Compound **19** was prepared as described above to provide the title compound as an off-white solid (71%). ¹H NMR (DMSO-*d*₆, 400 MHz): δ 0.4–0.5 (m, 2H), 0.7–0.8 (m, 2H), 1.3 (s, 9H), 2.5–2.6 (m, 1H), 3.0 (s, 3H), 3.7 (s, 3H), 6.7 (d, 1H, *J* = 9 Hz), 7.2 (d, 1H, *J* = 2 Hz), 7.4 (d, 1H, *J* = 2 Hz), 7.5–7.6 (m, 3H), 7.9 (dd, 1H, *J* = 6, 2 Hz), 8.0 (d, 1H, *J* = 9 Hz), 8.3 (s, 1H), 8.7 (d, 1H, *J* = 2 Hz), 9.2 (s, 1H), 10.1 (s, 1H), 10.3 (s, 1H). HPLC purity: system A, *t*_R 9.42 min (99%). ESMS *m/z* = 608 [M + H]⁺.

7-[(6-Cyclopropylamino-pyridine-3-carbonyl)-amino]-1-methyl-indole-2-carboxylic Acid (5-*tert*-Butyl-3-methanesulfonylamino-2-methoxy-phenyl)-amide (20): Compound **20** was prepared as described above (45%, off-white solid). ¹H NMR (DMSO-*d*₆, 400 MHz): δ 0.4–0.5 (m, 2H), 0.7–0.8 (m, 2H), 1.2 (s, 9H), 2.5–2.6 (m, 1H), 3.0 (s, 3H), 3.7 (s, 3H), 4.0 (s, 3H), 6.6 (d, 1H, *J* = 9 Hz), 7.1–7.2 (m, 2H), 7.3 (d, 1H, *J* = 2 Hz), 7.4 (s, 1H), 7.5 (d, 1H, *J* = 2 Hz), 7.6 (d, 1H, *J* = 2 Hz), 7.7 (dd, 1H, *J* = 7, 2 Hz), 8.0 (d, 1H, *J* = 7 Hz), 8.7 (d, 1H, *J* = 2 Hz), 9.1 (s, 1H), 9.8 (s, 1H), 10.0 (s, 1H). HPLC purity: system A, *t*_R 9.33 min (99%), system B, *t*_R 3.18 min (99%). ESMS *m/z* = 605 [M + H]⁺. Anal. Calcd for C₃₁H₃₆N₃O₅S: C, 61.57; H, 6.00; N, 13.90. Found: C, 61.11; H, 5.94; N, 13.46.

***N*-[2-(5-*tert*-Butyl-3-methanesulfonylamino-2-methoxy-phenylcarbamoyl)-benzo[*b*]thiophen-7-yl]-6-(cyclopropylmethyl-amino)-nicotinamide (21):** Compound **21** was prepared as described above (68%, off-white solid). ¹H NMR (DMSO-*d*₆, 400 MHz): δ 0.2–0.3 (m, 2H), 0.4–0.5 (m, 2H), 1.0–1.1 (m, 1H), 1.2 (s, 9H), 3.0 (s, 3H), 3.1–3.2 (m, 2H), 3.7 (s, 3H), 4.0 (s, 3H), 6.5 (d, 1H, *J* = 9 Hz), 7.2 (d, 1H, *J* = 2 Hz), 7.3 (s, 1H), 7.4 (d, 1H, *J* = 2 Hz), 7.5–7.6 (m, 2H), 7.8 (dd, 1H, *J* = 2, 7 Hz), 7.9 (d, 1H, *J* = 9 Hz), 8.3 (s, 1H), 8.7 (d, 1H, *J* = 2 Hz), 9.2 (s, 1H), 10.1 (s, 1H), 10.2 (s, 1H). HPLC purity: system A, *t*_R 9.63 min (99%). ESMS *m/z* = 622 [M + H]⁺. Anal. Calcd for C₃₁H₃₅N₅O₅S₂: C, 59.88; H, 5.67; N, 11.26. Found: C, 59.47; H, 5.65; N, 11.14.

7-[(6-(Cyclopropylmethyl-amino)-pyridine-3-carbonyl)-amino]-1-methyl-indole-2-carboxylic Acid (5-*tert*-Butyl-3-methanesulfonylamino-2-methoxy-phenyl)-amide (22): Compound **22** was prepared as described above (63%, off-white solid). ¹H NMR (DMSO-*d*₆, 400 MHz): δ 0.2–0.3 (m, 2H), 0.4–0.5 (m, 2H), 0.9–1.0 (m, 1H), 1.2 (s, 9H), 3.0 (s, 3H), 3.2 (t, 2H, *J* = 6 Hz), 3.7 (s, 3H), 4.0 (s, 3H), 6.5 (d, 1H, *J* = 9 Hz), 7.0–7.1 (m, 2H), 7.2 (d, 1H, *J* = 2 Hz), 7.3–7.4 (m, 2H), 7.5 (d, 1H, *J* = 2 Hz), 7.6 (dd, 1H, *J* = 7, 2 Hz), 7.9 (dd, 1H, *J* = 7, 2 Hz), 8.6 (d, 1H, *J* = 2 Hz), 9.1 (s, 1H), 9.8 (s, 1H), 10.0 (s, 1H). HPLC purity: system A, *t*_R 9.67 min (98%). ESMS *m/z* = 619 [M + H]⁺.

***N*-[2-(5-*tert*-Butyl-3-methanesulfonylamino-2-methoxy-phenylcarbamoyl)-benzo[*b*]thiophen-7-yl]-6-(2-methoxy-ethylamino)-nicotinamide (23):** Compound **23** was prepared as described above (55%, off-white solid). ¹H NMR (DMSO-*d*₆, 400 MHz): δ 1.2 (s, 9H), 3.1 (s, 3H), 3.3 (s, 3H), 3.4–3.5 (m, 4H), 3.7 (s, 3H), 6.6 (d, 1H, *J* = 9 Hz), 7.2 (d, 1H, *J* = 2 Hz), 7.3 (s, 1H), 7.4 (d, 1H, *J* = 2 Hz), 7.5–7.6 (m, 2H), 7.8 (dd, 1H, *J* = 6, 2 Hz), 7.9 (dd, 1H, *J* = 9, 2 Hz), 8.3 (s, 1H), 8.7 (d, 1H, *J* = 2 Hz), 9.2 (s, 1H), 10.1 (s, 1H), 10.3 (s, 1H). HPLC purity: system A, *t*_R 9.13 min (98%). ESMS *m/z* = 626 [M + H]⁺. Anal. Calcd for C₃₀H₃₅N₅O₆S₂: C, 57.58; H, 5.64; N, 11.19. Found: C, 57.60; H, 5.61; N, 10.92.

7-[(6-(2-Methoxy-ethylamino)-pyridine-3-carbonyl)-amino]-1-methyl-indole-2-carboxylic Acid (5-*tert*-Butyl-3-methanesulfonylamino-2-methoxy-phenyl)-amide (24): Compound **24** was prepared as described above (50%, off-white solid). ¹H NMR

(DMSO- d_6 , 400 MHz): δ 1.2 (s, 9H), 3.0 (s, 3H), 3.2 (s, 3H), 3.4–3.5 (m, 4H), 3.7 (s, 3H), 4.0 (s, 3H), 6.4 (d, 1H, $J = 9$ Hz), 7.0–7.1 (m, 2H), 7.2 (d, 1H, $J = 2$ Hz), 7.3 (s, 1H), 7.5 (d, 1H, $J = 2$ Hz), 7.6 (d, 1H, $J = 7$, 2 Hz), 7.9 (d, 1H, $J = 9$ Hz), 8.3 (s, 1H), 8.7 (d, 1H, $J = 2$ Hz), 9.1 (s, 1H), 9.8 (s, 1H), 10.0 (s, 1H). HPLC purity: system A, t_R 9.18 min (96%), system B, t_R 3.25 min (96%). ESMS $m/z = 623$ [M + H] $^+$.

In Vitro Methods. 1. Thermal Denaturation Assay: The details of the thermal denaturation experiments are found in ref 16. Briefly, the UV thermal melt experiments were carried out using a Perkin-Elmer Lambda 40 spectrophotometer. For each measurement, a quartz cuvette was loaded with 2.5 μ M murine p38 MAP kinase and 25 μ M inhibitor in a pH 7.0 buffer containing 10 mM sodium phosphate, 100 mM NaCl, and 1 mM TCEP. Absorbance data at 230 nm was collected as the temperature was scanned from 25 to 80 °C at a ramp rate of 0.2 °C/min. The melting temperature for each sample was calculated as the maximum deflection point of the first derivative of the melting transition using the Perkin-Elmer Templab software (version 1.62). Generally, the reported T_m values have an average standard error of ± 0.5 °C and are the average of at least two experiments unless otherwise noted. The T_m values can be converted into K_d values using the equation $T_m = 3.08(\log K_a) + 31.2$, where $K_a = 1/K_d$. The error associated with K_d calculations using this equation is $\pm 16\%$. It must be noted that this equation was developed for pyrazole naphthyl urea-based inhibitors (e.g., **1**) and if the thermodynamics of binding for this class of inhibitors is significantly different this relationship may be more of an approximation.

2. Human Whole Blood TNF-(HWB) Assay: This assay, performed in 96-well polypropylene plates, measures the ability of test compounds to inhibit the elaboration of TNF- α by human whole blood following ex vivo stimulation with LPS (*Escherichia coli* lipopolysaccharide 0111:B4). Each test well contained the following components: 15 μ L of compound serially diluted in human type AB serum, 135 μ L of freshly drawn heparinized human whole blood, and 15 μ L of LPS diluted in PBR S containing 10% human serum for a final concentration of 50 ng LPS/mL. The plates were incubated for 30 min at 37 °C prior to addition of LPS. Control wells on every plate contained no test compound, both with and without LPS. Following addition of LPS to test and control wells, the plates were placed on a rotary shaker for 30 s and then incubated for 5 h at 37 °C. To harvest plasma, 100 μ L of PBR S was added to all wells, the plates centrifuged to pellet cells, and the diluted plasma removed for TNF α quantitation by standard ELISA, DELFIA, or electrochemiluminescence assay methods. TNF α in each test well was determined by signal interpolation from a TNF α standard curve run on the same plate. Test compound EC₅₀ values were determined by nonlinear curve fitting of the data from cross-plate duplicate 11-point concentration–response curves to a 4-parameter logistic equation. Composite EC₅₀ values were the geometric mean of EC₅₀ values determined in blood from at least three donors. The EC₅₀ of a standard inhibitor was determined on 239 independent test days across 113 different blood donors and returned lower and upper one-standard deviation values that were 29 and 37% of the geometric mean EC₅₀ value.

In Vivo Methods. 1. LPS Challenge Assay: Female Balb/c mice, weighing approximately 20 g, were used. Mice were administered test compound in cremophor by oral gavage (volume of 0.15 mL) approximately 30 min prior to LPS/D-gal administration. Then, mice were administered LPS (*E. coli* LPS 0111:B4, 1.0 μ g/mouse) plus D-gal (50 mg/kg) intravenously in 0.2 mL of pyrogen-free saline. After 1 h, each mouse was anesthetized, and blood was collected by cardiac puncture for serum TNF α and compound level determinations. Blood samples were centrifuged at 2500 rpm for 10–15 min, the serum was decanted, and plasma concentration was determined by HPLC. The concentration of TNF- α in the serum was measured by a commercially available ELISA kit (R&D Systems, Minneapolis, MN). ELISA was performed according to the manufacturers assay procedure. All samples were assayed in duplicate.

2. Rat Pharmacokinetic Assessment: Male Sprague–Dawley

rats were placed into two groups of three animals per group. The animals were fasted overnight prior to dosing and food was returned approximately 4 h post-dose. The animals in group 1 were dosed via an intravenous injection into the femoral vein catheter (~15 s push) at a target dose level of 1 mg/kg for each compound and at a dose volume of 1 mL/kg. Immediately following dosing, each catheter was flushed with 0.5 mL of saline and tied off to prevent re-access. The animals in group 2 were dosed via oral gavage at a target dose of 10 mg/kg and a dose volume of 10 mL/kg. The plasma samples, dose formulation samples, and residual dose formulations were analyzed in a noncompartmental pharmacokinetic manner using WinNonlin Anal. Calc'd for software.

Acknowledgment. The authors are indebted to Dr. Mathew Netherton for critical reading of the manuscript.

References

- (1) Imajo, M.; Tsuchiya, Y.; Nishida, E. Regulatory mechanisms and functions of MAP kinase signaling pathways. *IUBMB Life* **2006**, *58* (5–6), 312–317.
- (2) Wagner, G.; Laufer, S. Small molecular anti-cytokine agents. *Med. Res. Rev.* **2005**, *26* (11), 1–62. (b) Calcagni, F.; Elenkov, I. Stress system activity, innate and T helper cytokines, and susceptibility to immune-related diseases. *Ann. N.Y. Acad. Sci.* **2006**, 62–76.
- (3) Klinkhoff, A. Biological agents for rheumatoid arthritis: Targeting both physical function and structural damage. *Drugs* **2004**, *64* (12), 1267–1283. (b) Barry, J.; Kirby, B. Novel biologic therapies for psoriasis. *Expert Opin. Biol. Ther.* **2004**, *6*, 975–987. (c) Elliott, M. J.; Maini, R. N.; Feldmann, M.; Kalden, J. R.; Antoni, C.; Smolen, J. S.; Leeb, B.; Breedveld, F. C.; Macfarlane, J. D.; Woody, J. N. Randomized double-blind comparison of chimeric monoclonal antibody to tumor necrosis factor α (cA2) versus placebo in rheumatoid arthritis. *Lancet* **1994**, *344*, 1105–1110. (d) Cohen, S. B.; Woolley, J. M. Interleukin 1 receptor antagonist anakinra improves functional status in patients with RA. *J. Rheumatol.* **2003**, *30*, 225–231. (e) Boehncke W. H.; Prinz, J.; Gottlieb, A. B. Biologic therapies for psoriasis. A systematic review. *J. Rheumatol.* **2006**, *33* (7), 1447–1451.
- (4) Saklatvala, J. The p38 MAP kinase pathway as a therapeutic target in inflammatory disease. *Curr. Opin. Pharmacol.* **2004**, *4* (4), 372–377.
- (5) Ashwell, J. D. The many paths to p38 mitogen-activated protein kinase activation in the immune system. *Nat. Rev. Immunol.* **2006**, *6* (7), 532–540.
- (6) Pargellis, C.; Tong, L.; Churchill, L.; Cirillo, P. F.; Gilmore, T.; Graham, A. G.; Grob, P. M.; Hickey, E. R.; Moss, N.; Pav, S.; Regan, J. Inhibition of p38 MAP kinase by utilizing a novel allosteric binding site. *Nat. Struct. Biol.* **2002**, *9* (4), 268–272.
- (7) (a) Dominguez, C.; Powers, D.; Tamayo, N. p38 MAP kinase inhibitors: Many are made, but few are chosen. *Curr. Opin. Drug Discovery Dev.* **2005**, *8*, 421–430. (b) Cirillo P. F.; Pargellis, C.; Regan, J. The non-diaryl heterocycle classes of p38 MAP kinase inhibitors. *Curr. Top. Med. Chem.* **2002**, *2* (9), 1021–1035.
- (8) Sullivan, J.; Holdgate, G. A.; Campbell, D.; Timms, D.; Gerhardt, S.; Breed, J.; Breeze, A. L.; Birmingham, A.; Pauptit, R. A.; Norman, R. A.; Embrey, K.; Read, J. Prevention of MKK6-dependent activation by binding to p38 α MAP kinase. *Biochemistry* **2005**, *44*, 16475–16490.
- (9) (a) Schindler, T.; Bornmann, W.; Pellicena, P.; Miller, W. T.; Clarkson, B.; Kuriyan, J. Structural mechanism for STI-571 inhibition of Abelson tyrosine kinase. *Science* **2000**, *289* (5486), 1938–1942. (b) Nagar, B.; Bornmann, W. G.; Pellicena, P.; Schindler, T.; Veach, D. R.; Miller, W. T.; Clarkson, B.; Kuriyan, J. Crystal structures of the kinase domain of c-Abl in complex with the small molecule inhibitors PD173955 and imatinib (STI-571). *Cancer Res.* **2002**, *62*, 4236–4243. (c) Tokarski, J. S.; Newitt, J. A.; Chang, C. Y. J.; Cheng, J. D.; Wittekind, M.; Kiefer, S. E.; Kish, K.; Lee, F. Y. F.; Borzilleri, R.; Lombardo, L. J.; Xie, D.; Zhang, Y.; Klei, H. E. The structure of Dasatinib (BMS-354825) bound to activated ABL kinase domain elucidates its inhibitory activity against Imatinib-resistant ABL mutants. *Cancer Res.* **2006**, *66*, 5790–5797.
- (10) Regan, J.; Capolino, A.; Cirillo, P. F.; Gilmore, T.; Graham, A. G.; Hickey, E.; Kroe, R. R.; Madwed, J.; Moriaki, M.; Nelson, R.; Pargellis, C. A.; Swinamer, A.; Torcellini, C.; Tsang, M.; Moss, N. Structure-activity relationships of the p38 α MAP kinase inhibitor 1-(5-*tert*-butyl-2-*p*-tolyl-2H-pyrazol-3-yl)-3-[4-(2-morpholin-4-yl-ethoxy)naphthalen-1-yl]urea (BIRB 796). *J. Med. Chem.* **2003**, *46* (22), 4676–4686.

- (11) Niculescu-Duvaz, I.; Roman, E.; Whittaker, S. R.; Friedlos, F.; Kirk, R.; Scanlon, I. J.; Davies, L. C.; Niculescu-Duvaz, D.; Marais, R.; Springer, C. J. Novel inhibitors of bRAF based on a disubstituted pyrazine scaffold. Generation of a nanomolar lead. *J. Med. Chem.* **2006**, *49* (1), 407–416.
- (12) Cirillo, P. F.; Hickey, E. Discovery of the *N*-phenyl-*N'*-naphthylurea class of p38 MAP kinase inhibitors. Results to be published at a later date.
- (13) Dominguez, C.; Tamayo, N.; Zhang, D. p38 Inhibitors: Beyond pyridinylimidazoles. *Expert Opin. Ther. Pat.* **2005**, *15* (7), 801–816.
- (14) Wang, R.; Gao, Y.; Lai, L. LigBuilder: A multi-purpose program for structure-based drug design. *J. Mol. Model.* **2000**, *6*, 498–516.
- (15) Rahaman, L. K. A.; Scowston, R. A. 7-Substituted benzo[*b*]-thiophenes and 1,2-benzisothiazoles. Part 2. Chloro and nitro derivatives. *J. Chem. Soc., Perkin Trans. 1* **1984**, *19*, 385–387.
- (16) For this series, a 2.8 °C change in thermal denaturation temperature corresponds to approximately a 10-fold change in binding affinity. However, it must be noted that this equation was developed for pyrazole naphthyl urea-based inhibitors (e.g., **1**), and if the thermodynamics of binding for this class of inhibitors is significantly different, this relationship may be more of an approximation. Kroe, R. R.; Regan, J.; Proto, A.; Peet, G. W.; Roy, T.; Dickert, L.; Fuschetto, N.; Pargellis, C. A.; Ingraham, R. H. Thermal denaturation: A method to rank slow binding, high-affinity p38a MAP kinase inhibitors. *J. Med. Chem.* **2003**, *46* (22), 4669–4675.
- (17) (a) Liu, C.; Wroblewski, S. T.; Lin, J.; Ahmed, G.; Metzger, A.; Wityak, J.; Gillooly, K. M.; Shuster, D. J.; McIntyre, K. W.; Pitt, S.; Shen, D. R.; Zhang, R. F.; Zhang, H.; Doweyko, A. M.; Diller, D.; Henderson, I.; Barrish, J. C.; Dodd, J. H.; Schieven, G. L.; Leftheris, K. 5-Cyanopyrimidine derivatives as a novel class of potent, selective, and orally active inhibitors of p38 α MAP kinase. *J. Med. Chem.* **2005**, *48* (20), 6261–6270. (b) Johnson, L. N.; De Moliner, E.; Brown, N. R.; Song, H.; Barford, D.; Endicott, J. A.; Noble, M. E. Structural studies with inhibitors of the cell cycle regulatory kinase cyclin-dependent protein kinase 2. *Pharmacol. Ther.* **2002**, *93* (2–3), 113–124.
- (18) Liverton, N. J.; Butcher, J. W.; Claiborne, C. F.; Claremon, D. A.; Libby, B. E.; Nguyen, K. T.; Pitzenberger, S. M.; Selnick, H. G.; Smith, G. R.; Tebben, A.; Vacca, J. P.; Varga, S. L.; Agarwal, L.; Dancheck, K.; Forsyth, A. J.; Fletcher, D. S.; Frantz, B.; Hanlon, W. H.; Harper, C. F.; Hofsess, S. J.; Kostura, M.; Lin, J.; Luell, S.; O'Neill, E. A.; Orevillo, C. J.; Pang, M.; Parsons, J.; Rolando, A.; Sahly, Y.; Visco, D. M.; O'Keefe, S. J. Design and synthesis of potent, selective, and orally bioavailable tetrasubstituted imidazole inhibitors of p38 mitogen-activated protein kinase. *J. Med. Chem.* **1999**, *42* (12), 2180–2190.
- (19) Carter, T. A.; Wodicka, L. M.; Shah, N. P.; Velasco, A. M.; Fabian, M. A.; Treiber, D. K.; Milanov, Z. V.; Atteridge, C. E.; Biggs, W. H., III; Edeen, P. T.; Floyd, M.; Ford, J. M.; Grotzfeld, R. M.; Herrgard, S.; Insko, D. E.; Mehta, S. A.; Patel, H. K.; Pao, W.; Sawyers, C. L.; Varmus, H.; Zarrinkar, P. P.; Lockhart, D. J. Inhibition of drug-resistant mutants of ABL, KIT, and EGF receptor kinases. *Proc. Natl. Acad. Sci. U.S.A.* **2005**, *102* (31), 11011–11016.

JM070415W